

SURFACE TENSION AND MACHINE COMPLIANCE EFFECTS ON CAVITY GROWTH IN SOFT MATERIALS

**Vijayanand Muralidharan¹, Chung-Yuen Hui¹, Josef Dollhofer², Costantino Creton²,
Yu Yun Lin³**

¹Department of Theoretical and Applied Mechanics, Cornell University, Ithaca, NY 14853 (vm45@cornell.edu, ch45@cornell.edu)

²Laboratoire Physique et Chimie Structurale et Macromoléculaire à l'Ecole Supérieure de Chimie et Physique Industrielles, Paris. (Josef.Dollhofer@espci.fr, Costantino.Creton@espci.fr)

³Department of Civil Engineering, National Cheng Kung University, Tainan, 701, Taiwan. (cyulin@mail.ncku.edu.tw)

Introduction

The formation and growth of cavities in incompressible hyperelastic solids is relevant to the understanding of Tackiness in Pressure Sensitive Adhesives (PSA). The classical problem of cavitation has been studied in great detail under constant traction conditions [1-2]. The focus of this work differs from previous studies in three main aspects, namely, a) the role of surface tension, b) the effect of the compliance of the loading machine, and c) the effect of different material models (Neo-Hookean and Mooney-Rivlin material models in particular).

We show that, for a Neo-Hookean material, the equilibrium solution is determined by three dimensionless parameters for the dead loading case and four parameters for the finite compliance case. Depending on the values of these parameters, multiple equilibrium solutions can exist. Specifically, there can be three equilibrium solutions for some sets of parameters. Two of these solutions are stable as they correspond to local energy minima. One of these stable solutions corresponds to cavity constriction (i.e., the cavity decreases in size) and the other to cavity expansion. Our model is compared with experimental results obtained in the context of probe tack tests of soft adhesives. We also consider the effects of material hardening and finite compliance.

Problem Description

We model the initial stage of a tack test where the adhesive layer is locally under nearly hydrostatic tension and cavities start to appear in the elastomer. The system is idealized to be composed of two parts, a spherical shell of material surrounding the cavity and the region external to this shell, which is modeled as linear springs connected to a rigid loading device. Initially, because of the low modulus of PSA's (typically in the 0.01-0.1MPa range), we consider the outer surface of the spherical shell to be under dead loading and the cavity under the action of surface tension forces.

Formulation

Consider a spherical cavity of undeformed radius A inside a spherical shell of radius B . The external surface is subjected to a dead load F , so that the traction P in the undeformed configuration is $F/4\pi B^2$. Assuming spherically symmetric deformations, the hoop stretch λ is

$$\lambda = r(R)/R \quad (1)$$

where R, r denote the distance of a material point from the center in the reference and current configuration respectively. The incompressibility condition imposes:

$$r(R) = (R^3 - A^3 + a^3)^{1/3} \quad (2)$$

where a is the deformed cavity radius. The normalized potential energy Π^* is

$$\Pi^* = U^* + U_\gamma^* - W_{ext}^* \quad (3)$$

where

$$U^* = (4\pi/E) \int_1^{B/A} w(R', A, a) R'^2 dR' \quad (4)$$

is the normalized strain energy,

$$U_\gamma^* = 4\pi\alpha\lambda_A^2 \quad (5)$$

is the normalized energy due to surface tension γ and

$$W_{ext}^* = 4\pi f^{-3} P^* \left[\left(1 + f^3 (\lambda_A^3 - 1) \right)^{1/3} - 1 \right] \quad (6)$$

is the normalized external work due to the dead load. All energies are normalized by EA^3 , where E is the infinitesimal Young's modulus of the elastomer. The dimensionless parameters f, α, P^* and λ_A are defined by

$$\alpha = \gamma/EA, f = A/B, P^* = P/E, \lambda_A = a/A \quad (7)$$

The strain energy densities w for the Neo-Hookean and Mooney-Rivlin materials are

$$w_{NH} = E(\lambda^{-4} + 2\lambda^2 - 3)/6 \quad (8a)$$

$$w_{MR} = c_{10}(\lambda^{-4} + 2\lambda^2 - 3) + c_{01}(\lambda^4 + 2\lambda^{-2} - 3) \quad (8b)$$

where c_{10} and c_{01} are material parameters. The equilibrium solution is obtained by enforcing the stationary condition i.e.

$$d\Pi^*(\lambda_A)/d\lambda_A \Big|_{\lambda_A=\lambda_A^*} = 0 \quad (9)$$

Dimensional considerations imply that the deformed cavity radius a must have the form:

$$a = A\phi(\alpha, P^*, f)$$

where ϕ is a dimensionless function.

Numerical Results

Surface tension becomes important when $\alpha > 1$, i.e. when $\gamma > EA$. For $\gamma = 30 \text{ mJ/m}^2$, $E = 0.05 \text{ MPa}$, this condition is satisfied for cavities with $A < 0.6 \mu\text{m}$. We present results for two cases, $A = 10 \mu\text{m}$ and $A = 0.5 \mu\text{m}$. For both the cases, $B = 50 \mu\text{m}$ i.e. $f = 0.2$ and 0.01 .

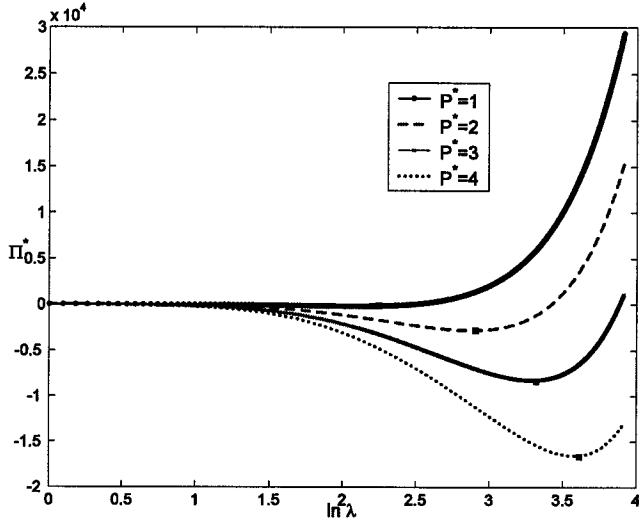


Figure 1. Plot of normalized Potential energy versus stretch at cavity surface for $f = 0.2$, $\alpha = 0.06$. Dots represent equilibrium solutions.

Figure 1 shows the potential energy plot for $f = 0.2$ for different applied loads. There is one equilibrium solution always, which corresponds to an energy minimum. Figures 2 and 3 show the same plot for $f = 0.01$ and it can be seen that for certain values of the applied load, there can be three solutions. The equilibrium solutions at a given nominal traction is summarized in Figure 4 for $f = 0.2$ and $f = 0.01$ cases. Due to space constraints, the results are not discussed in detail here and can be found in [4].

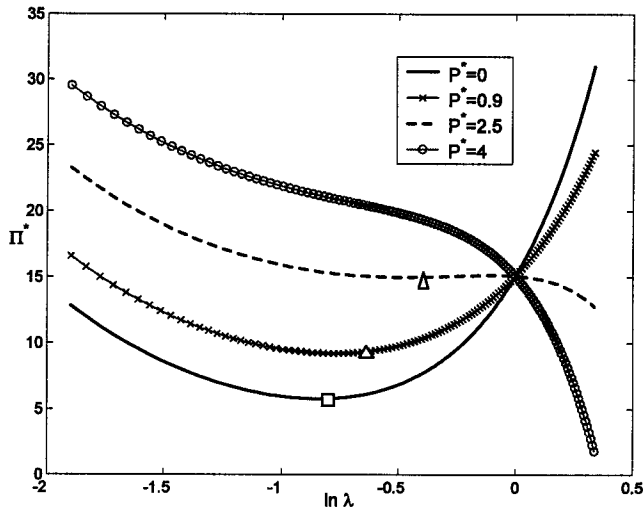


Figure 2. Plot of normalized Potential energy versus stretch at cavity surface for $f = 0.01$, $\alpha = 1.2$ and at $\lambda < 1$. Boxes and triangles represent global and local minima respectively.

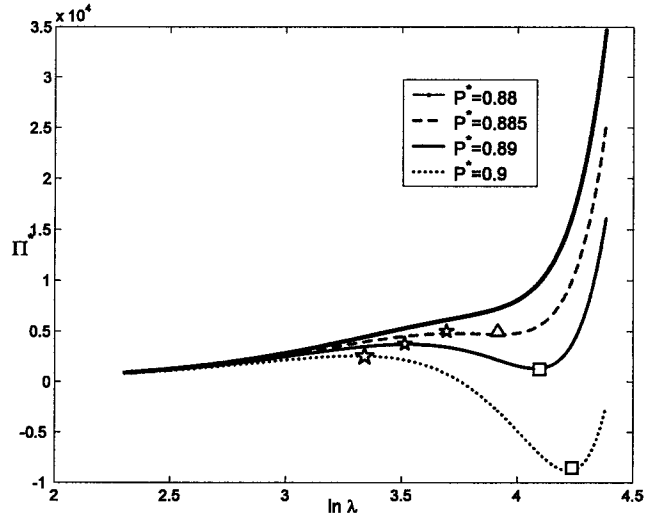


Figure 3. Plot of normalized Potential energy versus stretch at cavity surface for $f = 0.01$, $\alpha = 1.2$ showing multiple solutions at $\lambda > 1$. Boxes, triangles and stars represent global and local minima and local maxima respectively.

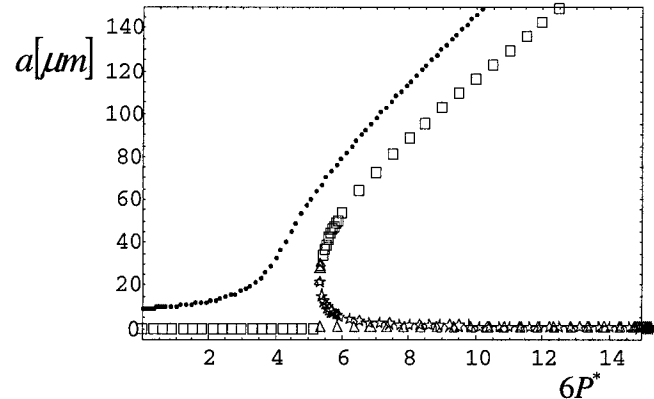


Figure 4. Deformed Cavity radius as a function of nominal stress for $f = 0.2$ (Dots represent global minima) and $f = 0.01$ (Boxes: global minima, triangles: local minima, stars: local maxima).

Experimental

The typical evolution of cavity radius with time as found in a tack test is shown in Figure 5 [5]. Since the force applied on the adhesive layer increases linearly with time, the time axis can be viewed as a load axis. One recognizes a continuous cavity growth for the optically visible large cavity marked (o). While there is no visible precursor for the cavity marked (x) at low loads, a cavity suddenly appears at medium loads and grows much more rapidly than the cavity originating from a visible precursor. The qualitative agreement between theory (Figure 4) and experiment

(Figure 5) is evident except for very large loads where cavity interaction is thought to be important and our simplified model for the growth of a single cavity does not apply.

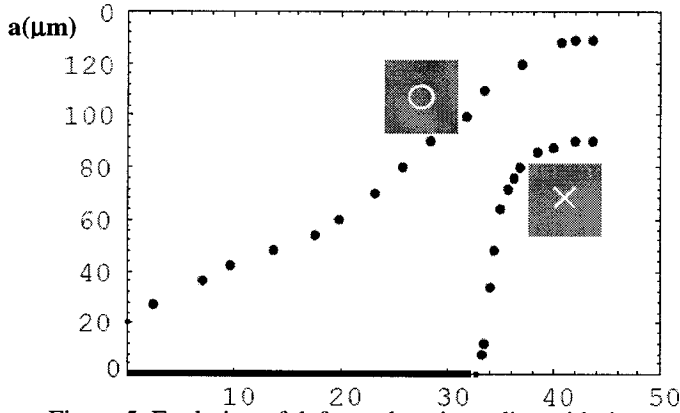


Figure 5. Evolution of deformed cavity radius with time, from an optically visible precursor (o) and without visible precursor (x).

Effect of Machine Compliance

To study the effect of machine compliance, we assume that the outer shell surface is connected by linear springs of stiffness k to a rigid loading device, which imposes a radial displacement δ . For the Neo-Hookean material, the exact solution in non-dimensional form can be written as

$$\frac{\delta}{A} = (\lambda_B - 1) \frac{B}{A} - \frac{8\pi\lambda_B^2 B^2 E}{3Ak} \left[\frac{1}{\lambda_A} + \frac{1}{\lambda_A^4} - \frac{1}{\lambda_B} - \frac{1}{\lambda_B^4} - \frac{3\gamma}{EA} \frac{1}{\lambda_A} \right] \quad (10)$$

where λ_B is the stretch at the outer surface. It can be shown that (10) reduces to the dead load case when $k \rightarrow 0$. When $k \rightarrow \infty$, the test is a displacement controlled one and the solution is always unique. We can easily identify four dimensionless parameters from (10), namely

$$\bar{\delta} = \frac{\delta}{A}, f = \frac{A}{B}, \beta = \frac{AE}{k}, \alpha = \frac{\gamma}{EA} \quad (11)$$

For a given set of parameters, the unknowns λ_A and λ_B can be determined using (10) and the incompressibility condition.

Case 1: $f = 0.2$, $\alpha = 0.06$

For all ranges of the parameters $\bar{\delta}$ and β , only one solution was found. This is to be expected since we obtained a unique solution for the limiting cases of load and displacement controlled tests and the result for the finite compliance case should be between these two limiting cases.

Case 2: $f = 0.01$, $\alpha = 1.2$

The results are summarized in Table 1. For three different values of the parameter β , two critical values of $\bar{\delta}$ were found. For $\bar{\delta} < \bar{\delta}_1$, there exists only one solution corre-

sponding to cavity constriction. For $\bar{\delta}_1 < \bar{\delta} < \bar{\delta}_2$, we have three solutions and beyond $\bar{\delta}_2$, we again have only one solution, corresponding to cavity expansion. In general, as the spring stiffness increases, the range of the parameter $\bar{\delta}$ for which multiple solutions exists decreases.

β	$\bar{\delta}_1$	$\bar{\delta}_2$
2.5×10^{-1}	2.78×10^4	8.24×10^4
2.5×10^{-3}	2.8×10^2	8.24×10^2
2.5×10^{-4}	28	82

Table 1. Critical values of $\bar{\delta}$ for different values of the parameter β .

Discussion and Conclusion

The role of surface tension was first considered by Gent and Tompkins [3] under constant traction conditions and they observed just one stable solution. We considered the effect of surface tension under dead loading and observed multiple solutions for certain parameter sets. It is to be emphasized here that the multiple stable solutions observed here are primarily due to the finite specimen size. Indeed, our formulation was extended to account for finite compliance effects and similar results were observed i.e. multiple solutions were found for some parameter sets.

The above analysis was also carried out for a Mooney-Rivlin material to study hardening effects. For values of c_{01}/E close to zero, the results are qualitatively similar to that of the Neo-Hookean material. As the value of this parameter increases, material hardening becomes significant and cavities are formed at progressively higher loads and only one stable solution was obtained.

Equilibrium solutions were also found by solving all the field equations and we obtained the same results as the energy approach outlined above. The role of viscoelasticity needs to be investigated and the above method based on solving the field equations is particularly well suited when we extend the above analysis to model viscoelastic effects.

References

1. R. Abeyaratne and Hang-Sheng Hou, *Journal of Elasticity*, 1991, **26**, pp 23-42.
2. J.M. Ball, *Philosophical Transactions of the Royal Society London*, 1982, **A306**, pp557-611.
3. A.N. Gent and D.A. Tompkins, *J. Polymer science, Part A2*, 1969, **7**, pp1483-1488.
4. J. Dollhofer, A.Chiche, Vijayanand Muralidharan, C. Creton and C.Y.Hui, 2003, *Submitted to Int. J. Sol. Struct.*
5. A. Chiche, J. Dollhofer and C. Creton. *Proceedings of the 27th Ann. Meeting of the Adhesion Society*, 2003.